Atmospheric
Chemistry
and Physics

Full latitudinal marine atmospheric measurements of iodine monoxide

Hisahiro Takashima[1,2], Yugo Kanaya[2], Saki Kato[1], Martina M. Friedrich[3], Michel Van Roozendael[3],
Fumikazu Taketani[2], Takuma Miyakawa[2], Yuichi Komazaki[2], Carlos A. Cuevas[4], Alfonso Saiz-Lopez[4],
and Takashi Sekiya[2]

[1]Faculty of Science, Fukuoka University, Fukuoka, Japan
[2]Japan Agency for Marine–Earth Science and Technology (JAMSTEC), Yokohama, Japan
[3]Belgian Institute for Space Aeronomy (BIRA-IASB), Brussels, Belgium
[4]Department of Atmospheric Chemistry and Climate, Institute of Physical
Chemistry Rocasolano (CSIC), Madrid, Spain

Correspondence: Hisahiro Takashima (hisahiro@fukuoka-u.ac.jp) and Yugo Kanaya (yugo@jamstec.go.jp)

Abstract. Iodine compounds destroy ozone (O_3) in the global troposphere and form new aerosols, thereby affecting the global radiative balance. However, few reports have described the latitudinal distribution of atmospheric iodine compounds. This work reports iodine monoxide (IO) measurements taken over unprecedented sampling areas from the Arctic to the Southern Hemisphere and spanning sea surface temperatures (SSTs) of approximately 0 to 31.5 °C. The highest IO concentrations were observed over the Western Pacific warm pool (WPWP), where O_3 minima were also measured. There, a negative correlation was found between O_3 and IO mixing ratios at extremely low O_3 concentrations. This correlation is not explained readily by the O_3-dependent oceanic fluxes of photolabile inorganic iodine compounds, which is the dominant source in recent global-scale chemistry transport models representing iodine chemistry. Actually, the correlation rather implies that O_3-independent pathways can be similarly important in the WPWP. The O_3-independent fluxes result in a 15 % greater O_3 loss than that estimated for O_3-dependent processes alone. The daily O_3 loss rate related to iodine over the WPWP is as high as approximately 2 ppbv (parts per billion by volume) despite low O_3 concentrations of approximately 10 ppbv, with the loss being up to 100 % greater than that without iodine. This finding suggests that warming SST driven by climate change might affect the marine atmospheric chemical balance through iodine–ozone chemistry.

1 Introduction

Halogens play an important role in tropospheric and stratospheric chemistry through the catalytic destruction of ozone (O_3), which affects the atmosphere's oxidizing capacity and the radiative balance of the Earth (Alicke et al., 1999; Koenig et al., 2020; Read et al., 2008; Saiz-Lopez et al., 2012, 2014; Simpson et al., 2015). Iodine, particularly, is potentially important in tropospheric chemistry because of its rapid reactions, although its concentration in the troposphere is low compared to that of chlorine and bromine. Iodine also forms aerosol particles; it can, thereby, affect the global radiative

balance (O'Dowd et al., 2002; Sipila et al., 2016; Gómez-Martín et al., 2020; Baccarini et al., 2020; Gómez-Martín et al., 2021; He et al., 2021).

Because of their low concentrations in the atmosphere, iodine compounds are difficult to quantify. Few reports have attempted to clarify their regional- to global-scale sources and roles in atmospheric chemistry (Großmann et al., 2013; Mahajan et al., 2012; Prados-Roman et al., 2015a; Dix et al., 2013; Volkamer et al., 2015). In the past, the primary source of iodine in the troposphere has long been regarded as organic compounds in coastal areas (Davis et al., 1996; Carpen-

ter et al., 2012; Prados-Roman et al., 2015a). However, the results of recent studies suggest that iodine compounds over the open ocean are emitted from inorganic sources following O_3 deposition over the ocean surface (Carpenter et al., 2013; Macdonald et al., 2014; Prados-Roman et al., 2015b). The inorganic sources are now regarded as the dominant emission term over the oligotrophic oceans in the global-scale chemistry transport models representing iodine chemistry (e.g., Saiz-Lopez et al., 2014; Sekiya et al., 2020), although the emission process of inorganic iodine is still insufficiently clear in more recent studies (e.g., Inamdar et al., 2020).

This study specifically examines iodine monoxide (IO) in the marine boundary layer over the open ocean from the wide latitudinal bands. Specifically, we examine processes occurring over the tropical Western Pacific, where the global sea surface temperature (SST) reaches a maximum (warm pool) and where O_3 minima have been reported (Rex et al., 2014; Kanaya et al., 2019; Kley et al., 1996). Actually, IO observations in environments with SSTs of $> 30\,°C$ are limited. Observations of IO have been made in the tropics but only for short time periods, with SST $> 30\,°C$, if any (Großmann et al., 2013; Dix et al., 2013; Prados-Roman et al., 2015a). Although the importance of halogen chemistry as a driver of O_3 losses in this region has been suggested (Großmann et al., 2013; Koenig et al., 2017), this point has yet to be examined in the context of full latitudinal distributions.

The initial production of atmospheric inorganic iodine species has not been fully examined in an environment where extremely low O_3 concentrations ($< 10\,ppb$ – parts per billion) are observed. Over the Atlantic Ocean (in Cabo Verde), long-term observations of iodine and ozone have been conducted, but they were in higher O_3 environments of approximately $20\,ppbv$ (parts per billion by volume; Read et al., 2008). We, therefore, examined IO variations over the tropical Western Pacific and their potential contributions to regional O_3 losses, with an emphasis on SST as a potential key parameter controlling the initial iodine emissions. The global SST maximum is observed in the tropical Western Pacific, but observations reported from earlier studies were only taken in the regions surrounding the maximum (Großmann et al., 2013; Prados-Roman et al., 2015a). Investigation of iodine variations in the tropics is also important for elucidating the stratospheric chemical balance (Koenig et al., 2017) because transport from the troposphere to the stratosphere occurs through the tropical tropopause layer (Takashima et al., 2008; Saiz-Lopez et al., 2015; Koenig et al., 2017; Holton et al., 1995). In fact, it is particularly important over the tropical Western Pacific.

For this study, using the multi-axis differential optical absorption spectroscopy (MAX–DOAS) remote sensing technique, IO observations were made to quantify IO concentrations over the open ocean, covering the widest latitudinal range ever examined with a single instrument. The technique uses scattered solar radiation at several elevation angles to obtain atmospheric aerosol and gas profile concentrations (Hönninger et al., 2004; Wagner et al., 2004; Wittrock et al., 2004; Sinreich et al., 2005; Frieß et al., 2006; Kanaya et al., 2014). MAX–DOAS generally measures trace gas contents over a long light path (up to 10–$20\,km$) at low elevation angles. The long light path enables the detection of low concentrations of species of interest at near-surface altitudes. MAX–DOAS is, therefore, useful for quantifying low-abundance tropospheric trace gases, such as IO, over the open ocean.

Multi-platform measurements by MAX–DOAS from aircraft (Koenig et al., 2017; Volkamer et al., 2009) and ships (Großmann et al., 2013; Takashima et al., 2012; Volkamer et al., 2009) have been developed in recent years. Earlier studies have retrieved IO concentrations (typically $< 1\,pptv$ – parts per trillion by volume) in the marine boundary layer over the open ocean from shipboard MAX–DOAS measurements (Großmann et al., 2013; Mahajan et al., 2012; Prados-Roman et al., 2015a; Inamdar et al., 2020). Since 2008, the Japan Agency for Marine–Earth Science and Technology (JAMSTEC) has undertaken an unprecedented set of MAX–DOAS measurements on board the research vessels (R/Vs) *Kaiyo*, *Mirai*, and *Kaimei* around the world (Takashima et al., 2012). This report presents IO and O_3 variations over the open ocean from the Arctic to the Southern Hemisphere as observed on R/V *Mirai* between 2014–2018.

2   Methodology

2.1   Iodine monoxide observations from ship-based MAX–DOAS measurements

The shipboard MAX–DOAS apparatus used for this study comprised two main components, i.e., an outdoor telescope and an indoor UV–Vis spectrometer (SP-2358 coupled to a PIXIS 400B back-illuminated CCD (charge-coupled device) detector; Acton Research Corporation and Teledyne Princeton Instruments, respectively). These were connected using a 10–$14\,m$ long fiber-optic cable ($100\,\mu m$ radius; 60 core or 40 core). The telescope unit was developed jointly by the Japan Agency for Marine–Earth Science and Technology (JAMSTEC) and Prede Co., Ltd. (Tokyo, Japan). The movable prism of the telescope unit rotates for elevation angles (ELs) of 3, 5, 10, 30, and $90°$. The EL is changed every minute to observe scattered sunlight. The target EL is attained by adjusting the angle of the prism actively and by considering the angle of the ship's roll (Takashima et al., 2016). The telescope line of sight was off the starboard side of the ship, with a field of view of approximately $1.0°$. The spectrometer was housed in an adiabatic plastic box, with the temperature held constant at $35\,°C \pm 0.1\,°C$ using a temperature controller (KT4; Panasonic Inc., Japan). The CCD was cooled to $-70\,°C$. The spectrometer was equipped with a 600 line per millimeter grating at $300\,nm$. The slit width was $100\,\mu m$. The typical exposure time was 0.1–$0.2\,s$.
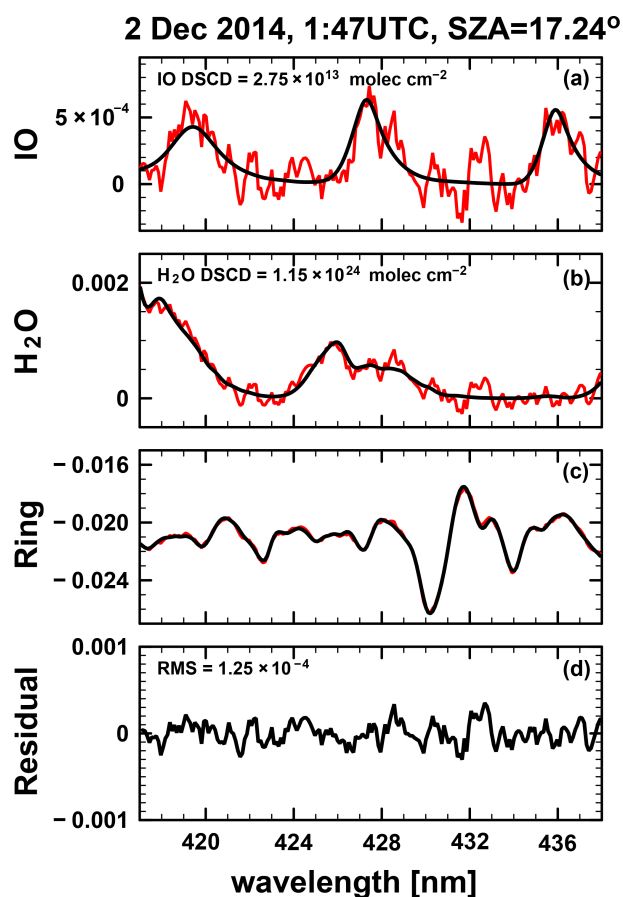
2 Dec 2014, 1:47UTC, SZA=17.24°

Figure 1. Nonlinear least squares spectral fitting results for IO concentrations observed on 2 December 2014. Panels **(a)** and **(b)** show the fitting for IO and H_2O. Black lines represent the cross section scaled to the spectrum (red) determined by differential optical absorption spectroscopy. Panels **(c)** and **(d)** show the Ring effect contribution and the residual spectrum.

Figure 2. Time series of IO and H_2O differential slant column densities (DSCDs) for elevation angles of 3, 5, 10, 20, 30, and 90°, the root mean square residual, and the solar zenith angle observed on 1–2 December 2014 over the tropical Western Pacific.

Table 1. Cross sections of iodine monoxide (IO) and O_4 differential slant column densities used for this study.

	Component	Reference
IO	NO_2	Vandaele et al. (1998)
	O_3	Bogumil et al. (2000)
	H_2O	HITEMP* (Rothman et al., 2013)
	IO	Gómez-Martín et al. (2005)
O_4	NO_2	Vandaele et al. (1998)
	O_3	Bogumil et al. (2000)
	H_2O	HITEMP (Rothman et al., 2013)
	O_4	Thalman and Volkamer (2013)

* Correction factors from Lampel et al. (2015) were applied.

Spectral data were selected for analysis when the EL was within ±0.5° of the target. Data were analyzed using the DOAS method (Platt and Stutz, 2008). A nonlinear least squares spectral fitting procedure was used to derive differential slant column densities (DSCDs) of the oxygen collision complex (O_2–O_2 or O_4) and IO using the QDOAS software package (Danckaert et al., 2017), for which the absorption cross section data presented in Table 1 were used. For O_4 and IO retrievals, 425–490 and 415–438 nm fitting windows were applied, respectively. Examples of fitting results and the time series of DSCDs are presented, respectively, in Figs. 1 and 2. The typical fitting error of the IO DSCDs was approximately 1×10^{12} molec. cm^{-2}, with a detection limit of approximately 4×10^{12} molec. cm^{-2} (2σ).

The Mexican MAX-DOAS Fit (MMF) retrieval algorithm (Friedrich et al., 2019) was used for the retrieval of IO profiles and vertical column densities. The version of MMF used in this study is the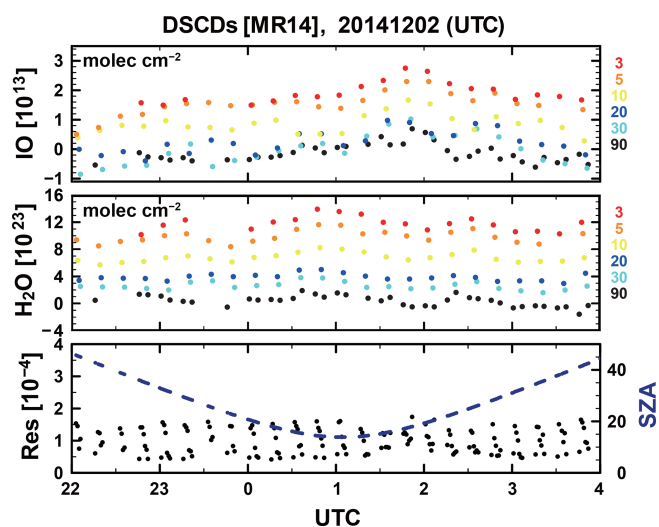 same as used in Frieß et al. (2019) and Tirpitz et al. (2021) but with adjusted a priori and variance–covariance matrix settings to fit for IO retrieval. MMF applies the optimal estimation method and uses a two-step approach in which the aerosol profile is first retrieved from O_4 DSCDs. Then, the IO profile is retrieved from the IO DSCDs, using the earlier retrieved aerosol profile in the forward model. We used VLIDORT (v.2.7; Spurr, 2006) as the forward model in a pseudo-spherical multiple-scattering setting. Only intensity information and its analytically calculated Jacobians were used. No other Stokes parameter was used. MMF was used in logarithmic retrieval space on a retrieval grid of up to 4 km with a 200 m layer height.

Both a priori profiles were constructed as constant below 500 m, with an exponentially decreasing profile above 500 m for aerosol and IO profiles, to examine near-surface areas specifically. The a priori aerosol optical depth was set as 0.18. The a priori IO vertical column density (VCD) was

set to 2.5×10^{12} molec. cm^{-2}. The a priori covariance matrix S_a for both aerosol and IO retrieval was constructed using the square of 100 % of the a priori profile on the diagonal and a correlation length of 200 m. For the aerosols, the only retrieved quantity was the partial aerosol optical depth per layer. Therefore, in the forward model, a constant single scattering albedo of 0.95 was used for both retrievals, i.e., aerosol and IO. The phase function moments were constructed using the Henyey–Greenstein phase function (Henyey and Greenstein, 1941) with a constant asymmetry factor of 0.72. The surface albedo in the forward models was set as 0.06. Here, the single scattering albedo, asymmetry factor, and surface albedo were used, similar to the work presented by Großmann et al. (2013). The degrees of freedom (DOF) for the IO retrieval for MR14-06 (leg1) were 1–1.4. Typical averaging kernels for IO are presented in Fig. S1 in the Supplement. It is also noteworthy that the observed IO contents might be a little low compared to those from earlier studies conducted over the open ocean because of inaccuracy of the water–vapor cross section used in earlier retrievals (Lampel et al., 2015).

2.2 Zero-dimensional photochemical box model with iodine chemistry

A zero-dimensional photochemical box model (Kanaya et al., 2007a, b), based on the Regional Atmospheric Chemistry Mechanism (RACM; Stockwell et al., 1997) and custom iodine chemistry, was updated to include 91 chemical species and 275 reactions (reactions of iodine chemistry added to RACM are presented in Table 3). It was used to simulate the time evolution of mixing ratios of O_3 (initially 18 ppbv) and iodinated species in the boundary layer with an assumed height of 500 m over the equatorial Pacific region, where the maximum concentrations of IO and minimum concentrations of O_3 were observed. For O_3, dry deposition at a velocity of 0.04 cm s^{-1} was considered (Pound et al., 2020). An entrainment flux of 1.2×10^8 molec. $cm^{-2} s^{-1}$ was assumed for NO_2, for which the initial mixing ratio was assumed to be 15 pptv. Fluxes of hypoiodous acid (HOI) and I_2 from the ocean surface were estimated, respectively (Carpenter et al., 2013), as 8.4×10^7 and 2.6×10^6 molec. $cm^{-2} s^{-1}$ at 10 ppbv of O_3, for an aqueous I^- concentration of 74 nM and wind speed of 5 m s^{-1} (8.9×10^7 molec. $cm^{-2} s^{-1}$ as total HOI/I_2 ($=$ HOI $+ 2I_2$) flux). The I^- concentration was referred from the nearest observation data at 12° N and 158° E (Tsunogai and Henmi, 1971). The assumed wind speed was from observations made during MR14-06 cruise over the region. For Case 1a, the fluxes were assumed to be linearly dependent on O_3, which is consistent with Carpenter et al. (2013). For Case 1b, a 25 % reduction in the flux was assumed, potentially because of the presence of a sea surface microlayer or dissolved organic matter (Hayase et al., 2010, 2012; Shaw and Carpenter, 2013; Tinel et al., 2020). The blue band of Fig. 3 represents the range of Cases 1a
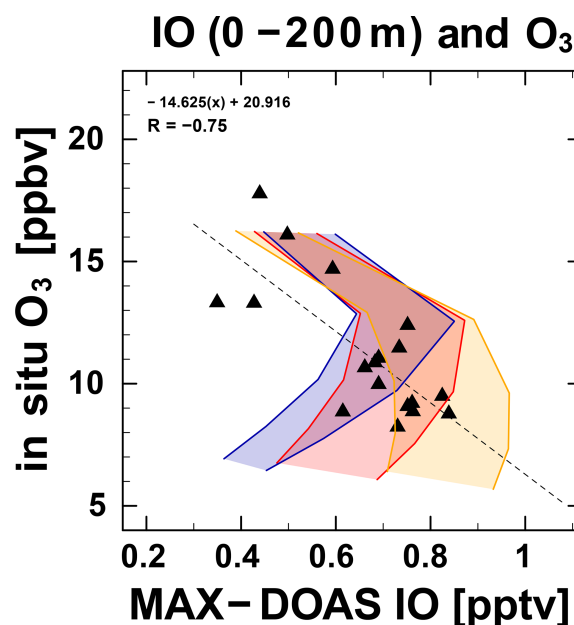

Figure 3. Daily median IO mixing ratio for 0–200 m (pptv) observed by MAX–DOAS versus daily median in situ ozone mixing ratio (ppbv). Results of box model simulations with O_3-dependent (Case 1), quasi-O_3-dependent (Case 2), and pure O_3 independent (Case 3) emission fluxes of iodine compounds are superimposed respectively as blue, red, and orange shaded areas.

and 1b, representing the case with O_3-dependent fluxes. In Cases 2a and 2b, the O_3-dependent flux in Case 1a was reduced to half and compensated by O_3-independent inorganic iodine fluxes of 3.3 (or 6.6) $\times 10^7$ molec. $cm^{-2} s^{-1}$ (red band of Fig. 3, which represents the quasi-O_3-dependent case). As a reference, a hypothetical case (Cases 3a and 3b) with a purely O_3-independent flux of the magnitude of 9.9 (or 13) $\times 10^7$ molec. $cm^{-2} s^{-1}$ was also tested (orange band of Fig. 3, which represents the purely O_3-independent case). The time-dependent simulations continued for 5 d, with the evaluation of the mixing ratio of O_3 and its relation with IO involving daytime averages (06:00–18:00 ship local time) over the first to fourth days. Dry deposition velocities of iodine species (I, IO, HI, HOI, OIO, I_2O_2, INO, INO_2, $IONO_2$, and I_2) were assumed to be 1 cm s^{-1}.

2.3 Backward trajectory calculation

The origins of air masses over the tropical Western Pacific were investigated using 5 d backward trajectory calculations (Takashima et al., 2011) based on meteorological analysis data of the European Centre for Medium-Range Weather Forecasts (ECMWF).

2.4 In situ gas measurements

For measurements of O_3 and CO, ambient air was sampled using approximately 20 m of Teflon tubing (6.35 mm outer

Table 2. Reactions of iodine chemistry added to RACM.

Reactants	Products	A (cm^3 molec.$^{-1}$ s^{-1})	E_a/R (K)	Reference
I + O$_3$	IO + O$_2$	2.10×10^{-11}	830	Atkinson et al. (2007), Sherwen et al. (2016)
I + HO$_2$	HI + O$_2$	1.50×10^{-11}	1090	Atkinson et al. (2007), Sherwen et al. (2016)
IO + NO	I + NO$_2$	7.15×10^{-12}	-300	Atkinson et al. (2007), Sherwen et al. (2016)
IO + HO$_2$	HOI + O$_2$	1.40×10^{-11}	-540	Atkinson et al. (2007), Sherwen et al. (2016)
IO + IO	0.43OIO + 0.71I + 0.43I$_2$O$_2$	9.60×10^{-11}	0	Stutz et al. (1999)
OH + HI	I + H$_2$O	1.60×10^{-11}	-440	Atkinson et al. (2007), Sherwen et al. (2016)
HOI + OH	IO + H$_2$O	5.00×10^{-12}	0	Riffault et al. (2005), Sherwen et al. (2016)
I + NO$_3$	IO + NO$_2$	4.50×10^{-10}	0	Chambers et al. (1992), McFiggans et al. (2000)
IO + CH$_3$O$_2$	0.25I + 0.254HCHO + 0.25HO$_2$+ 0.75HOI + 0.746ORA1 + 0.004H$_2$O$_2$	1.00×10^{-11}	0	Stutz et al. (1999)
IO +$h\nu$	I + O$_3$			Harwood et al. (1997), Kanaya et al. (2007b)
HOI +$h\nu$	I + OH			Rowley et al. (1999), Kanaya et al. (2007b)
INO$_2$ +$h\nu$	0.5I + 0.5NO$_2$ + 0.5IO + 0.5NO			Sander et al. (2011), McFiggans et al. (2000), Kanaya et al. (2007b)
IONO$_2$ +$h\nu$	0.5IO + 0.5NO$_2$ + 0.5I + 0.5NO$_3$			Sander et al. (2011), McFiggans et al. (2000), Kanaya et al. (2007b)
OIO + OH	HOI + O$_2$	7.00×10^{-12}	0	Von Glasow (2000), Kanaya et al. (2007b)
I$_2$O$_2$ +$h\nu$	I + OIO			Davis et al. (1996), Kanaya et al. (2007b)
I + NO$_2$ (+M)	INO$_2$ (+M)	5.40×10^{-12}	0	Alicke et al. (1999), Atkinson et al. (2007), Kanaya et al. (2003)
INO$_2$	I + NO$_2$	$9.94 \times 10^{+17}$	11 859	McFiggans et al. (2000), Sherwen et al. (2016)
IO + NO$_2$ (+M)	IONO$_2$ (+M)	3.70×10^{-12}	0	Alicke et al. (1999), Atkinson et al. (2007), Kanaya et al. (2003)
IONO$_2$	IO + NO$_2$	$2.10 \times 10^{+15}$	13 670	Kaltsoyannis and Plane (2008), Sherwen et al. (2016)
I + NO (+M)	INO (+M)	4.10×10^{-13}	0	Alicke et al. (1999), Atkinson et al. (2007), Kanaya et al. (2003)
INO	I + NO	1.40×10^{-1}	0	Alicke et al. (1999), Kanaya et al. (2003)
OIO + NO	IO + NO$_2$	1.10×10^{-12}	-542	Atkinson et al. (2007), Sherwen et al. (2016)
IO + ISOP	0.25I + 0.132MACR + 0.855OLT + 0.25HO$_2$+ 0.179HCHO + 0.75HOI + 0.075H$_2$O$_2$+ 0.9OH	1.00×10^{-11}	0	Analogous to Stutz et al. (1999), Kanaya et al. (2007b)
IBr +$h\nu$	I			Seery and Britton (1964), Kanaya et al. (2007b)
OIO +$h\nu$	I + O$_2$			McFiggans et al. (2000), Kanaya et al. (2007c)
I$_2$ + OH	HOI + I	2.10×10^{-10}		Atkinson et al. (2007), Sherwen et al. (2016)
I$_2$ + NO$_3$	I + IONO$_2$	1.50×10^{-12}		Atkinson et al. (2007), Sherwen et al. (2016)
I$_2$ +$h\nu$	2I			Tellinghuisen (1973), Alicke et al. (1999)
IO + OIO	I$_2$O$_3$	1.5×10^{-10}		Gómez Martín et al. (2007), Sherwen et al. (2016)
OIO + OIO	I$_2$O$_4$	1.5×10^{-10}		Gómez Martín et al. (2007), Sherwen et al. (2016)
I$_2$O$_2$	OIO + I	1.13		Kaltsoyannis and Plane (2008), Galvez et al. (2013), Gómez Martín and Plane (2009), Saiz-Lopez et al. (2016)
I$_2$O$_2$	IO + IO	0.00532		Kaltsoyannis and Plane (2008), Galvez et al. (2013), Gómez Martín and Plane (2009), Saiz-Lopez et al. (2016)
I$_2$O$_4$	OIO + OIO	0.0879		Kaltsoyannis and Plane (2008), Gómez Martín and Plane (2009), Saiz-Lopez et al. (2016)
HOI + NO$_3$	IO + HNO$_3$	$2.7 \times 10^{-12} \times (300/T)^{2.66}$		Saiz-Lopez et al. (2016)
I$_2$O$_3$ +$h\nu$	IO + OIO			Saiz-Lopez et al. (2014, 2016)
I$_2$O$_4$ +$h\nu$	OIO + OIO			Saiz-Lopez et al. (2014, 2016)

Table 3. Research cruises of the R/V *Mirai* that generated the data used for this study.

Cruise	Period	Area
MR14-06 (leg 1)	8 Nov–3 Dec 2014	Western Pacific; tropics
MR15-04	6–21 Nov 2015	Western Pacific; eastern Indian Ocean
MR15-05 (leg 2)	14–24 Jan 2016	Western Pacific
MR16-06	24 Aug–4 Oct 2016	Arctic Ocean; Bering Sea; North Pacific
MR16-09 (leg 3)	8 Feb–3 Mar 2017	Southern Ocean
MR17-05C	25 Aug–29 Sep 2017	Arctic Ocean; Bering Sea; North Pacific
MR17-08	22 Nov 2017–17 Jan 2018	Western Pacific; eastern Indian Ocean

diameter) from the bow (Kanaya et al., 2019). To avoid contamination from ship exhaust, 1 min data that deviated more than 1σ from the hourly discrete average were deleted. The typical magnitude of 1σ over the remote ocean was approximately 0.1–0.5 ppbv. The O_3 and CO concentrations were measured, respectively, using UV and infrared absorptions with O_3 and CO monitors (49C and 48C; Thermo Scientific, USA). The O_3 instrument was calibrated twice per year in the laboratory, before and after deployment, using a primary standard O_3 generator. The CO instrument was calibrated on board twice per year, on embarking and disembarking of the instrument, using a premixed standard gas. The reproducibility of the calibration was to within 1 % for O_3 and 3 % for CO (Kanaya et al., 2019). The O_3 concentrations observed from R/V *Mirai* cruises, presented in Table 3, are shown in Fig. S2.

3   Results and discussion

The IO contents (differential slant column densities (DSCDs) for an elevation angle of 3°) observed from R/V *Mirai* during seven research cruises during 2014–2018 are presented in Fig. 4. The cruises are presented in Table 3. Although observations were limited to some seasons and years (e.g., Arctic measurements were limited to the Northern Hemisphere summer), whole latitudinal bands were covered from 74° N to 67° S, and strong latitudinal variations in IO concentrations were observed, with a maximum detected clearly in the tropics (10° S–10° N) but not at higher latitudes in either hemisphere. Over Southeast Asia (near Indonesia), high IO concentrations were sometimes observed near coastal areas. The highest values of up to approximately 2×10^{13} molec. cm^{-2} (DSCD) were also observed in the tropical Western Pacific, with wide variations in global SST maxima ($> 30\,^\circ$C). From similar earlier studies (Gómez-Martín et al., 2013; Großmann et al., 2013; Mahajan et al., 2012), no data obtained under very high SST conditions over a long period were reported. Therefore, our IO observations at SST maxima (up to 31.5 °C), and during more than 2 weeks, represent the most comprehensive measurements of reactive iodine over the tropical Western Pacific warm pool (WPWP).
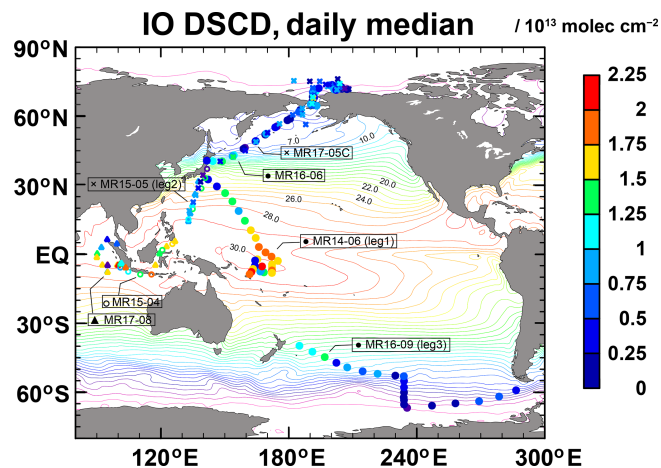

Figure 4. Daily median IO content (DSCDs for an elevation angle of 3°; molec. cm^{-2}) observed from the R/V *Mirai* during 2014–2018. Color contours represent the optimum interpolated SST averaged for 2014–2018.

Specifically regarding IO variations over the tropical Western Pacific, we found IO VCDs of approximately 0.7–1.8×10^{12} molec. cm^{-2} (Fig. 5). The 5 d backward trajectories indicate that air masses in this region originated from the open ocean (Fig. 5). The carbon monoxide (CO) content was constantly low (60 ppbv; Fig. 6), which is also consistent with an air mass originating from the open ocean. In addition, the chlorophyll content, based on satellite MODIS measurements (MODIS-Aqua, MODISA, Level 3 version 2018) in the source region, was also low (Fig. 5), implying that any organic source of iodine can be expected to be negligible (although we also must consider abiotic organic source and mesotrophic conditions; Jones et al., 2010). The IO data collected over the tropical Western Pacific are consistent with I^- variations reported in earlier studies (Chance et al., 2014, 2019; Sherwen et al., 2016), indicating an increase in I^- concentration with SST.

For the time series of IO concentrations near the ocean surface (0–200 m height; Fig. 7), the values were approximately 0.3–0.8 pptv, with wide variations over a timescale of a few days. The IO concentration near the surface depends on the shape of the a priori profile used for the re-
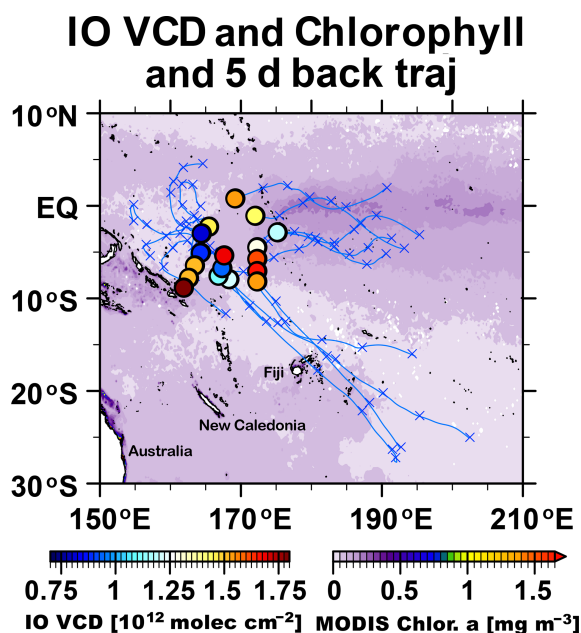
IO VCD and Chlorophyll and 5 d back traj

Figure 5. Daily median tropospheric IO vertical column densities (VCDs; molec. cm^{-2}) observed from R/V *Mirai* during 16 November to 2 December 2014 and chlorophyll *a* concentrations observed via satellite (MODIS). Blue crosses and lines represent 5 d backward trajectories.
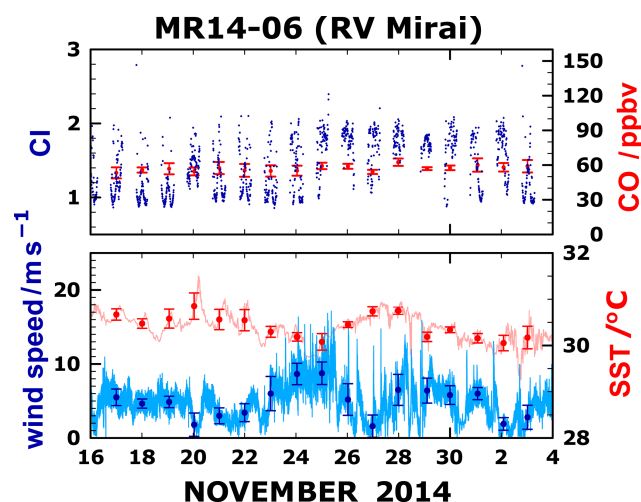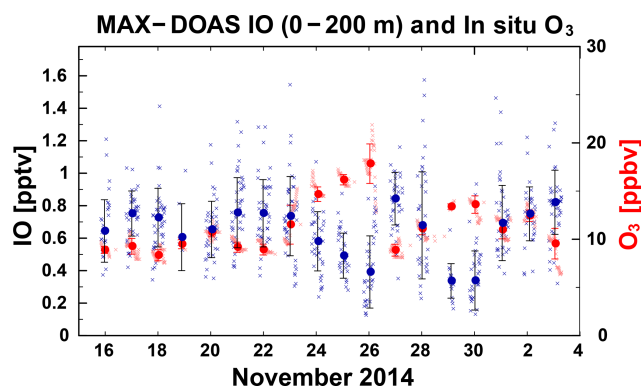

Figure 6. Time series of the CO mixing ratio (ppbv), color index (CI; defined as the ratio of the measured intensities at the two wavelengths of 500 and 380 nm; Takashima et al., 2009), wind speed (m s^{-1}), and SST (°C).

trieval, but day-to-day variations near the surface were unaffected by the choice of profile. Insufficient data were retrieved to document diurnal IO variations accurately. At times, the O_3 concentrations were generally low (< 20 ppbv) and extremely low (< 10 ppbv; Fig. 7). One unique finding was that, even under low-O_3 conditions, a negative correlation was found between IO and O_3 concentrations in the daily dataset (Figs. 3 and 7). Laboratory studies indicate that high O_3 concentrations can cause emissions of iodine from ocean to atmosphere (Carpenter et al., 2013; Macdonald et al., 2014; Sakamoto et al., 2009). This O_3-dependent iodine release has been regarded as being more dominant than other O_3-independent types of emissions, including photolabile iodocarbons such as CH_2I_2, CH_2ICl, and their subsequent photolysis over the open oceans in every global-scale chemistry transport model representing iodine chemistry (Saiz-Lopez et al., 2014; Sekiya et al., 2020; Sherwen et al., 2016). However, with an O_3-dependent HOI/I_2 flux of approximately 9×10^7 molec. cm^{-2} s^{-1} (Sect. 2.2), as expected under an O_3 mixing ratio of approximately 10 ppbv, a zero-dimensional box model was not able to reproduce the negative correlation found between IO and O_3. Because the initial HOI/I_2 release flux limited by O_3 in the < 12 ppbv mixing ratio range cannot drive the strong O_3 reduction, the scenario produced only a positive correlation (Case 1; Fig. 3). In contrast, another case, in which the O_3-independent flux was added to compensate for the O_3-dependent term weakened by a factor of 2 (Case 2; Fig. 3), better reproduced

the observed trend. The weakened flux might be explained by dissolved organic carbon (Shaw and Carpenter, 2013) or the presence of a sea surface microlayer (Tinel et al., 2020) impeding iodine vaporization. The added O_3-independent flux is not explainable solely by flux from the photolysis of iodocarbons within the marine boundary layer (approximately 10^7 molec. cm^{-2} s^{-1}) generally assumed in the three-dimensional models (Saiz-Lopez et al., 2014; Sekiya et al., 2020; Sherwen et al., 2016). While indirectly considering the global total fluxes of CH_2IX ($X = $ I, Br, and Cl), as described by Ordóñez et al. (2012) in these model simulations, the chl-*a*-based parameterization reduced the fluxes to too a low level over this oceanic region. It, therefore, necessitates a survey of missing sources. We might not need a brand new flux mechanism but, rather, a good parameterization of the traditional organoiodine fluxes (including their photolysis) over the region.

The third case, with only an O_3-independent flux (Case 3; Fig. 3) might explain the negative correlation more easily, whereas the total change of the flux type is simply not being supported. We, therefore, hypothesize that O_3-independent processes are more important than has been represented by recent models. Indeed, a larger magnitude of organic iodine flux (approximately 7×10^7 molec. cm^{-2} s^{-1}) was reported in the low-latitude Pacific (Großmann et al., 2013) and would, therefore, be the most likely cause of the negative correlation. However, that study (Großmann et al., 2013) relied on assumption of an even larger inorganic iodine emission flux to explain the observed IO concentrations. Therefore, our analysis is the first to suggest that the O_3-independent flux can be comparably important to the O_3-dependent flux in this region. Other O_3-independent iodine release mechanisms, such as photooxidation of aqueous I^- (Watanabe et

Table 4. Net and process-specific O_3 loss rates in three cases at an O_3 concentration of 10 ppbv, as calculated using the box model.

	IO (ppbv)	net loss (ppbv d^{-1})	HO$_x$/O$_x$ cycle loss (ppbv d^{-1})	Iodine cycle loss (ppbv d^{-1})
Without iodine	0	−1.06	−1.64	0
Case 1	0.553–0.741	−1.85 to −2.08	−1.62	−0.519 to −0.720
Case 2	0.611–0.851	−1.92 to −2.21	−1.62	−0.579 to −0.844
Case 3	0.723–0.960	−2.05 to −2.34	−1.62	−0.700 to −0.967

Figure 7. Time series of IO mixing ratio for 0–200 m (blue; pptv) observed by MAX–DOAS, and in situ O_3 mixing ratio (red; ppbv). Circles and horizontal bars, respectively, represent the daily median and 1 standard deviation.

al., 2019), might also be worth exploring. The modeled net O_3 loss rate attributable to iodine in Case 2 increased by up to 100 % over that without iodine. The O_3 loss rate in the iodine cycle in Case 2 increased by approximately 15 % over that in Case 1 (Table 4).

The expectation that a positive correlation between O_3 and IO would occur with O_3-dependent processes over a low O_3 concentration range was also confirmed using three-dimensional global chemistry transport models, including halogen chemistry (Sekiya et al., 2020; Saiz-Lopez et al., 2014), over the tropical Western Pacific (Figs. S3, S4). An alternative explanation for the observed negative correlation would be the mixing of air masses with different degrees of iodine chemistry. If so, such a negative correlation could appear in the chemistry transport model results. However, this feature was not found. Therefore, we propose an O_3-independent flux. Over the Atlantic, the O_3 mixing ratio rarely reaches these low levels (10 ppbv or fewer). Therefore, such process analyses have not been undertaken there. Under the influence of O_3-independent sources, even lower O_3 concentrations would be attainable. Radiative forcing of O_3, as estimated recently with halogen chemistry (Sherwen et al., 2017; Iglesias-Suarez et al., 2020; Saiz-Lopez et al., 2012; Hossaini et al., 2015), might be influenced by the dependence of iodine flux on O_3 concentration, which might play a major role in estimating past and future concentrations of O_3.

The time series of meteorological parameters including wind speed and SST was also investigated, but a clear correlation, such as that shown by O_3 and IO, was not observed in the correlation with O_3 or IO concentrations on a timescale of a few days (Fig. 6). The correlation coefficient between SST and IO was found to be 0.39, that between SST and O_3 was −0.51, and that between wind speed and IO was −0.45. In addition, that between wind speed and O_3 was 0.59. It is noteworthy that the correlation coefficient between IO and O_3 was −0.75, which is much higher than others and, therefore, is the dominant feature. An earlier study (Kanaya et al., 2019) investigating the diurnal variation of O_3 in this area based on a comparison of observational data and a chemical transport model indicated that an as-yet-unidentified O_3 loss might occur over the tropical Western Pacific. Our results imply that iodine chemistry plays an important role in O_3 loss in the area of SST maxima, which is regarded as an entry point from the troposphere to stratosphere. Moreover, these results provide insights into the manner by which increasing SST associated with climate change might modify the marine atmospheric chemical balance, which warrants further investigation. Results of recent studies indicate a roughly three-fold increase in iodine since the 1950s, with at least 50 % attributed to anthropogenic O_3 (Cuevas et al., 2018; Legrand et al., 2018; Zhao et al., 2019). If half of the inorganic flux were O_3-independent, as suggested by Case 2, then either some other cause should be sought or the change in O_3-dependent fluxes to produce the observed change is even more dramatic than previously thought. Further investigation of these points is necessary.

4 Summary

In this study, shipboard multi-axis differential optical absorption spectroscopy (MAX–DOAS), a remote sensing technique, was used during seven research cruises covering the widest latitudinal bands, from the Arctic to the Southern Hemisphere, ever made with a single instrument, spanning SSTs of approximately 0 to 31.5 °C and allowing the investigation of the variation of IO concentrations. It was particularly abundant over the tropical Western Pacific (warm pool), appearing as an iodine fountain, where SST maxima (> 30 °C) and O_3 minima are observed.

This report describes negative correlation between IO and O_3 concentrations over the IO maximum, even under extremely low O_3 conditions, which few earlier studies have demonstrated. This correlation is not explained easily by the O_3-dependent oceanic fluxes of photolabile inorganic iodine compounds adopted for recent simulation studies. Our findings rather imply that O_3-independent pathways which release iodine compounds from the ocean are also important. Iodine input to the atmosphere from the ocean surface is greater in areas of higher SST, leading to an iodine fountain in the Western Pacific warm pool because the I^- concentration in the ocean surface is likely to be higher in these areas. This higher concentration might contribute to more pronounced O_3 destruction over the Western Pacific warm pool than estimated earlier. Warming SSTs associated with climate change can change the atmospheric chemical balance through halogen chemistry, warranting further quantitative investigation.

Competing interests. At least one of the (co-)authors is a member of the editorial board of *Atmospheric Chemistry and Physics*. The peer-review process was guided by an independent editor, and the authors also have no other competing interests to declare.

Disclaimer. Publisher's note: Copernicus Publications remains neutral with regard to jurisdictional claims in published maps and institutional affiliations.

References

Alicke, B., Hebestreit, K., Stutz, J., and Platt, U.: Iodine oxide in the marine boundary layer, Nature, 397, 572–573, https://doi.org/10.1038/17508, 1999.

Atkinson, R., Baulch, D. L., Cox, R. A., Crowley, J. N., Hampson, R. F., Hynes, R. G., Jenkin, M. E., Rossi, M. J., and Troe, J.: Evaluated kinetic and photochemical data for atmospheric chemistry: Volume III – gas phase reactions of inorganic halogens, Atmos. Chem. Phys., 7, 981–1191, https://doi.org/10.5194/acp-7-981-2007, 2007.

Baccarini, A., Karlsson, L., Dommen, J., Duplessis, P., Vullers, J., Brooks, I. M., Saiz-Lopez, A., Salter, M., Tjernstrom, M., Baltensperger, U., Zieger, P., and Schmale, J.: Frequent new particle formation over the high Arctic pack ice by enhanced iodine emissions, Nat. Commun., 11, 4924, https://doi.org/10.1038/s41467-020-18551-0, 2020.

Bogumil, K., Orphal, J., and Burrows, J. P.: Temperature-dependent absorption cross-sections of O_3, NO_2, and other atmospheric trace gases measured using the SCIAMACHY spectrometer, Proceedings of the ERS-Envisat Symposium, October 2000, Goteborg, Sweden, 2000.

Carpenter, L. J., Archer, S. D., and Beale, R.: Ocean-atmosphere trace gas exchange, Chem. Soc. Rev., 41, 6473–6506, https://doi.org/10.1039/c2cs35121h, 2012.

Carpenter, L. J., MacDonald, S. M., Shaw, M. D., Kumar, R., Saunders, R. W., Parthipan, R., Wilson, J., and Plane, J. M. C.: Atmospheric iodine levels influenced by sea sur-

face emissions of inorganic iodine, Nat. Geosci., 6, 108–111, https://doi.org/10.1038/Ngeo1687, 2013.

Chambers, R. M., Heard, A. C., and Wayne, R. P.: Inorganic gas-phase reactions of the nitrate radical – $I_2 + NO_3$ and $I + NO_3$, J. Phys. Chem., 96, 3321–3331, 1992.

Chance, R., Baker, A. R., Carpenter, L., and Jickells, T. D.: The distribution of iodide at the sea surface, Environ. Sci.-Proc. Imp., 16, 1841–1859, https://doi.org/10.1039/c4em00139g, 2014.

Chance, R. J., Tinel, L., Sherwen, T., Baker, A. R., Bell, T., Brindle, J., Campos, M., Croot, P., Ducklow, H., Peng, H., Hopkins, F., Hoogakker, B., Hughes, C., Jickells, T. D., Loades, D., Macaya, D. A. R., Mahajan, A. S., Malin, G., Phillips, D., Roberts, I., Roy, R., Sarkar, A., Sinha, A. K., Song, X., Winkelbauer, H., Wuttig, K., Yang, M., Peng, Z., and Carpenter, L. J.: Global sea-surface iodide observations, 1967–2018, Sci. Data, 6, 286, https://doi.org/10.1038/s41597-019-0288-y, 2019.

Cuevas, C. A., Maffezzoli, N., Corella, J. P., Spolaor, A., Vallelonga, P., Kjaer, H. A., Simonsen, M., Winstrup, M., Vinther, B., Horvat, C., Fernandez, R. P., Kinnison, D., Lamarque, J. F., Barbante, C., and Saiz-Lopez, A.: Rapid increase in atmospheric iodine levels in the North Atlantic since the mid-20th century, Nat. Commun., 9, 1452, https://doi.org/10.1038/s41467-018-03756-1, 2018.

Danckaert, T., Fayt, C., Van Roozendael, M., De Smedt, I., Letocart, V., Merlaud, A., and Pinardi, G.: QDOAS software user manual, Belgian Institute for Space Aeronomy, https://uv-vis.aeronomie.be/software/QDOAS/QDOAS_manual.pdf (last access: 22 March 2022), 2017.

Davis, D., Crawford, J., Liu, S., McKeen, S., Bandy, A., Thornton, D., Rowland, F., and Blake, D.: Potential impact of iodine on tropospheric levels of ozone and other critical oxidants, J. Geophys. Res.-Atmos., 101, 2135–2147, https://doi.org/10.1029/95jd02727, 1996.

Dix, B., Baidara, S., Bresch, J. F., Hall, S. R., Schmidt, K. S., Wang, S. Y., and Volkamer, R.: Detection of iodine monoxide in the tropical free troposphere, P. Natl. Acad. Sci. USA, 110, 2035–2040, https://doi.org/10.1073/pnas.1212386110, 2013.

Friedrich, M. M., Rivera, C., Stremme, W., Ojeda, Z., Arellano, J., Bezanilla, A., García-Reynoso, J. A., and Grutter, M.: NO_2 vertical profiles and column densities from MAX-DOAS measurements in Mexico City, Atmos. Meas. Tech., 12, 2545–2565, https://doi.org/10.5194/amt-12-2545-2019, 2019.

Frieß, U., Monks, P. S., Remedios, J. J., Rozanov, A., Sinreich, R., Wagner, T., and Platt, U.: MAX-DOAS O_4 measurements: A new technique to derive information on atmospheric aerosols: 2. Modeling studies, J. Geophys. Res., 111, D14203, https://doi.org/10.1029/2005jd006618, 2006.

Frieß, U., Beirle, S., Alvarado Bonilla, L., Bösch, T., Friedrich, M. M., Hendrick, F., Piters, A., Richter, A., van Roozendael, M., Rozanov, V. V., Spinei, E., Tirpitz, J.-L., Vlemmix, T., Wagner, T., and Wang, Y.: Intercomparison of MAX-DOAS vertical profile retrieval algorithms: studies using synthetic data, Atmos. Meas. Tech., 12, 2155–2181, https://doi.org/10.5194/amt-12-2155-2019, 2019.

Galvez, O., Gomez Martin, J. C., Gomez, P. C., Saiz-Lopez, A., and Pacios, L. F.: A theoretical study on the formation of iodine oxide aggregates and monohydrates, Phys. Chem. Chem. Phys., 15, 15572–15583, https://doi.org/10.1039/C3CP51219C, 2013.

Gómez Martín, J. C. and Plane, J. M. C.: Determination of the O-IO bond dissociation energy by photofragment excitation spectroscopy, Chem. Phys. Lett., 474, 79–83, 2009.

Gómez-Martín, J. C., Spietz, P., and Burrows, J. P.: Spectroscopic studies of the I-2/O-3 photochemistry – Part 1: Determination of the absolute absorption cross sections of iodine oxides of atmospheric relevance, J. Photoch. Photobio. A, 176, 15–38, https://doi.org/10.1016/j.jphotochem.2005.09.024, 2005.

Gómez Martín, J. C., Spietz, P., and Burrows, J. P.: Kinetic and mechanistic studies of the I_2/O_3 photochemistry, J. Phys. Chem. A, 111, 306–320, https://doi.org/10.1021/jp061186c, 2007.

Gómez Martín, J. C., Mahajan, A. S., Hay, T. D., Prados-Román, C., Ordóñez, C., MacDonald, S. M., Plane, J. M. C., Sorribas, M., Gil, M., Paredes Mora, J. F., Agama Reyes, M. V., Oram, D. E., Leedham, E., and Saiz-Lopez, A.: Iodine chemistry in the eastern Pacific marine boundary layer, J. Geophys. Res.-Atmos., 118, 887–904, https://doi.org/10.1002/jgrd.50132, 2013.

Gómez-Martín, J. C., Lewis, T. R., Blitz, M. A., Plane, J. M. C., Kumar, M., Francisco, J. S., and Saiz-Lopez, A.: A gas-to-particle conversion mechanism helps to explain atmospheric particle formation through clustering of iodine oxides, Nat. Commun., 11, 4521, https://doi.org/10.1038/s41467-020-18252-8, 2020.

Gómez-Martín, J. C., Saiz-Lopez, A., Cuevas, C. A., Fernandez, R. P., Gilfedder, B. S., Weller, R., Baker, A. R., Droste, E., and Lai, S.: Spatial and temporal variability of iodine in aerosol, J. Geophys. Res.-Atmos., 126, e2020JD034410, https://doi.org/10.1002/essoar.10505416.1, 2021.

Großmann, K., Frieß, U., Peters, E., Wittrock, F., Lampel, J., Yilmaz, S., Tschritter, J., Sommariva, R., von Glasow, R., Quack, B., Krüger, K., Pfeilsticker, K., and Platt, U.: Iodine monoxide in the Western Pacific marine boundary layer, Atmos. Chem. Phys., 13, 3363–3378, https://doi.org/10.5194/acp-13-3363-2013, 2013.

Harwood, M. H., Burkholder, J. B., Hunter, M., Fox, R. W., and Ravishankara, A. R.: Absorption cross sections and self-reaction kinetics of the IO radical, J. Phys. Chem., 101, 853–863, 1997.

Hayase, S., Yabushita, A., Kawasaki, M., Enami, S., Hoffmann, M. R., and Colussi, A. J.: Heterogeneous Reaction of Gaseous Ozone with Aqueous Iodide in the Presence of Aqueous Organic Species, J. Phys. Chem. A, 114, 6016–6021, https://doi.org/10.1021/jp101985f, 2010.

Hayase, S., Yabushita, A., and Kawasaki, M.: Iodine Emission in the Presence of Humic Substances at the Water's Surface, J. Phys. Chem. A, 116, 5779–5783, https://doi.org/10.1021/jp2048234, 2012.

He, X. C., Tham, Y. J., Dada, L., Wang, M. Y., Finkenzeller, H., Stolzenburg, D., Iyer, S., Simon, M., Kurten, A., Shen, J. L., Rorup, B., Rissanen, M., Schobesberger, S., Baalbaki, R., Wang, D. S., Koenig, T. K., Jokinen, T., Sarnela, N., Beck, L. J., Almeida, J., Amanatidis, S., Amorim, A., Ataei, F., Baccarini, A., Bertozzi, B., Bianchi, F., Brilke, S., Caudillo, L., Chen, D. X., Chiu, R., Chu, B. W., Dias, A., Ding, A. J., Dommen, J., Duplissy, J., El Haddad, I., Carracedo, L. G., Granzin, M., Hansel, A., Heinritzi, M., Hofbauer, V., Junninen, H., Kangasluoma, J., Kemppainen, D., Kim, C., Kong, W. M., Krechmer, J. E., Kvashin, A., Laitinen, T., Lamkaddam, H., Lee, C. P., Lehtipalo, K., Leiminger, M., Li, Z. J., Makhmutov, V., Manninen, H. E., Marie, G., Marten, R., Mathot, S., Mauldin, R. L., Mentler, B., Mohler, O., Muller, T., Nie, W., Onnela, A., Petaja, T., Pfeifer, J., Philippov, M., Ranjithkumar, A., Saiz-

Lopez, A., Salma, I., Scholz, W., Schuchmann, S., Schulze, B., Steiner, G., Stozhkov, Y., Tauber, C., Tome, A., Thakur, R. C., Vaisanen, O., Vazquez-Pufleau, M., Wagner, A. C., Wang, Y. H., Weber, S. K., Winkler, P. M., Wu, Y. S., Xiao, M., Yan, C., Ye, Q., Ylisirnio, A., Zauner-Wieczorek, M., Zha, Q. Z., Zhou, P. T., Flagan, R. C., Curtius, J., Baltensperger, U., Kulmala, M., Kerminen, V. M., Kurten, T., Donahue, N. M., Volkamer, R., Kirkby, J., Worsnop, D. R., and Sipila, M.: Role of iodine oxoacids in atmospheric aerosol nucleation, Science, 371, 589–595, https://doi.org/10.1126/science.abe0298, 2021.

Henyey, L. G. and Greenstein, J. L.: Diffuse radiation in the Galaxy, Astrophys. J., 93, 70–83, https://doi.org/10.1086/144246, 1941.

Holton, J. R., Haynes, P. H., Mcintyre, M. E., Douglass, A. R., Rood, R. B., and Pfister, L.: Stratosphere-Troposphere Exchange, Rev. Geophys., 33, 403–439, https://doi.org/10.1029/95rg02097, 1995.

Hönninger, G., von Friedeburg, C., and Platt, U.: Multi axis differential optical absorption spectroscopy (MAX-DOAS), Atmos. Chem. Phys., 4, 231–254, https://doi.org/10.5194/acp-4-231-2004, 2004.

Hossaini, R., Chipperfield, M. P., Montzka, S. A., Rap, A., Dhomse, S., and Feng, W.: Efficiency of short-lived halogens at influencing climate through depletion of stratospheric ozone, Nat. Geosci., 8, 186–190, https://doi.org/10.1038/Ngeo2363, 2015.

Iglesias-Suarez, F., Badia, A., Fernandez, R. P., Cuevas, C. A., Kinnison, D. E., Tilmes, S., Lamarque, J. F., Long, M. C., Hossaini, R., and Saiz-Lopez, A.: Natural halogens buffer tropospheric ozone in a changing climate, Nat. Clim. Change, 10, 147–154, https://doi.org/10.1038/s41558-019-0675-6, 2020.

Inamdar, S., Tinel, L., Chance, R., Carpenter, L. J., Sabu, P., Chacko, R., Tripathy, S. C., Kerkar, A. U., Sinha, A. K., Bhaskar, P. V., Sarkar, A., Roy, R., Sherwen, T., Cuevas, C., Saiz-Lopez, A., Ram, K., and Mahajan, A. S.: Estimation of reactive inorganic iodine fluxes in the Indian and Southern Ocean marine boundary layer, Atmos. Chem. Phys., 20, 12093–12114, https://doi.org/10.5194/acp-20-12093-2020, 2020.

Jones, C. E., Hornsby, K. E., Sommariva, R., Dunk, R. M., Von Glasow, R., McFiggans, G., and Carpenter, L. J.: Quantifying the contribution of marine organic gases to atmospheric iodine, Geophys. Res. Lett., 37, L18804, https://doi.org/10.1029/2010gl043990, 2010.

JAMSTEC: MIRAI MR14-06 Leg1 Cruise Data, JAMSTEC [data set], https://doi.org/10.17596/0001862, 2015.

JAMSTEC: BPPT, MIRAI MR15-04 Cruise Data, JAMSTEC [data set], https://doi.org/10.17596/0001975, 2016a.

JAMSTEC: BPPT, MIRAI MR15-05 Leg2 Cruise Data, JAMSTEC [data set], https://doi.org/10.17596/0002030, 2016b.

JAMSTEC: MIRAI MR16-06 Cruise Data, JAMSTEC [data set], https://doi.org/10.17596/0001870, 2016c.

JAMSTEC: MIRAI MR16-09 Leg3 Cruise Data, JAMSTEC [data set], https://doi.org/10.17596/0000026, 2017a.

JAMSTEC: MIRAI MR17-05C Cruise Data, JAMSTEC [data set], https://doi.org/10.17596/0001879, 2017b.

JAMSTEC: MIRAI MR17-08 Leg1 Cruise Data, JAMSTEC [data set], https://doi.org/10.17596/0001881, 2018a.

JAMSTEC: MIRAI MR17-08 Leg2 Cruise Data, JAMSTEC [data set], https://doi.org/10.17596/0001882, 2018b.

Kaltsoyannis, N. and Plane, J. M. C.: Quantum chemical calculations on a selection of iodine-containing species (IO, OIO, INO$_3$, (IO)$_2$, I$_2$O$_3$, I$_2$O$_4$ and I$_2$O$_5$) of importance in the atmosphere, Phys. Chem. Chem. Phys., 10, 1723–1733, 2008.

Kanaya, Y., Kajii, Y., and Akimoto, H.: Solar actinic flux and photolysis frequency determinations by radiometers and a radiative transfer model at Rishiri Island: comparisons, cloud effects, and detection of an aerosol plume from Russian forest fires, Atmos. Environ., 37, 2463–2475, https://doi.org/10.1016/S1352-2310(03)00183-3, 2003.

Kanaya, Y., Cao, R. Q., Akimoto, H., Fukuda, M., Komazaki, Y., Yokouchi, Y., Koike, M., Tanimoto, H., Takegawa, N., and Kondo, Y.: Urban photochemistry in central Tokyo: 1. Observed and modeled OH and HO$_2$ radical concentrations during the winter and summer of 2004, J. Geophys. Res.-Atmos., 112, D21312, https://doi.org/10.1029/2007jd008670, 2007a.

Kanaya, Y., Tanimoto, H., Matsumoto, J., Furutani, H., Hashimoto, S., Komazaki, Y., Tanaka, S., Yokouchi, Y., Kato, S., Kajii, Y., and Akimoto, H.: Diurnal variations in H$_2$O$_2$, O$_3$, PAN, HNO$_3$ and aldehyde concentrations and NO/NO$_2$ ratios at Rishiri Island, Japan: Potential influence from iodine chemistry, Sci. Total Environ., 376, 185–197, https://doi.org/10.1016/j.scitotenv.2007.01.073, 2007b.

Kanaya, Y., Cao, R. Q., Kato, S. G., Miyakawa, Y. K., Kajii, Y., Tanimoto, H., Yokouchi, Y., Mochida, M., Kawamura, K., and Akimoto, H.: Chemistry of OH and HO$_2$ radicals observed at Rishiri Island, Japan, in September 2003: Missing daytime sink of HO$_2$ and positive nighttime correlations with monoterpenes, J. Geophys. Res.-Atmos., 112, D11308, https://doi.org/10.1029/2006jd007987, 2007c.

Kanaya, Y., Irie, H., Takashima, H., Iwabuchi, H., Akimoto, H., Sudo, K., Gu, M., Chong, J., Kim, Y. J., Lee, H., Li, A., Si, F., Xu, J., Xie, P.-H., Liu, W.-Q., Dzhola, A., Postylyakov, O., Ivanov, V., Grechko, E., Terpugova, S., and Panchenko, M.: Long-term MAX-DOAS network observations of NO2 in Russia and Asia (MADRAS) during the period 2007–2012: instrumentation, elucidation of climatology, and comparisons with OMI satellite observations and global model simulations, Atmos. Chem. Phys., 14, 7909–7927, https://doi.org/10.5194/acp-14-7909-2014, 2014.

Kanaya, Y., Miyazaki, K., Taketani, F., Miyakawa, T., Takashima, H., Komazaki, Y., Pan, X., Kato, S., Sudo, K., Sekiya, T., Inoue, J., Sato, K., and Oshima, K.: Ozone and carbon monoxide observations over open oceans on R/V *Mirai* from 67° S to 75° N during 2012 to 2017: testing global chemical reanalysis in terms of Arctic processes, low ozone levels at low latitudes, and pollution transport, Atmos. Chem. Phys., 19, 7233–7254, https://doi.org/10.5194/acp-19-7233-2019, 2019.

Kley, D., Crutzen, P. J., Smit, H. G. J., Vomel, H., Oltmans, S. J., Grassl, H., and Ramanathan, V.: Observations of near-zero ozone concentrations over the convective Pacific: Effects on air chemistry, Science, 274, 230–233, https://doi.org/10.1126/science.274.5285.230, 1996.

Koenig, T. K., Volkamer, R., Baidar, S., Dix, B., Wang, S., Anderson, D. C., Salawitch, R. J., Wales, P. A., Cuevas, C. A., Fernandez, R. P., Saiz-Lopez, A., Evans, M. J., Sherwen, T., Jacob, D. J., Schmidt, J., Kinnison, D., Lamarque, J.-F., Apel, E. C., Bresch, J. C., Campos, T., Flocke, F. M., Hall, S. R., Honomichl, S. B., Hornbrook, R., Jensen, J. B., Lueb, R., Montzka, D. D., Pan, L. L., Reeves, J. M., Schauffler, S. M., Ullmann, K., Weinheimer, A. J., Atlas, E. L., Donets, V., Navarro, M. A., Riemer,

D., Blake, N. J., Chen, D., Huey, L. G., Tanner, D. J., Hanisco, T. F., and Wolfe, G. M.: BrO and inferred Bry profiles over the western Pacific: relevance of inorganic bromine sources and a Bry minimum in the aged tropical tropopause layer, Atmos. Chem. Phys., 17, 15245–15270, https://doi.org/10.5194/acp-17-15245-2017, 2017.

Koenig, T. K., Baidar, S., Campuzano-Jost, P., Cuevas, C. A., Dix, B., Fernandez, R. P., Guo, H., Hall, S. R., Kinnison, D., Nault, B. A., Ullmann, K., Jimenez, J. L., Saiz-Lopez, A., and Volkamer, R.: Quantitative detection of iodine in the stratosphere, P. Natl. Acad. Sci. USA, 117, 1860–1866, https://doi.org/10.1073/pnas.1916828117, 2020.

Lampel, J., Frieß, U., and Platt, U.: The impact of vibrational Raman scattering of air on DOAS measurements of atmospheric trace gases, Atmos. Meas. Tech., 8, 3767–3787, https://doi.org/10.5194/amt-8-3767-2015, 2015.

Legrand, M., McConnell, J. R., Preunkert, S., Arienzo, M., Chellman, N., Gleason, K., Sherwen, T., Evans, M. J., and Carpenter, L. J.: Alpine ice evidence of a three-fold increase in atmospheric iodine deposition since 1950 in Europe due to increasing oceanic emissions, P. Natl. Acad. Sci. USA, 115, 12136–12141, https://doi.org/10.1073/pnas.1809867115, 2018.

MacDonald, S. M., Gómez Martín, J. C., Chance, R., Warriner, S., Saiz-Lopez, A., Carpenter, L. J., and Plane, J. M. C.: A laboratory characterisation of inorganic iodine emissions from the sea surface: dependence on oceanic variables and parameterisation for global modelling, Atmos. Chem. Phys., 14, 5841–5852, https://doi.org/10.5194/acp-14-5841-2014, 2014.

Mahajan, A. S., Gómez Martín, J. C., Hay, T. D., Royer, S.-J., Yvon-Lewis, S., Liu, Y., Hu, L., Prados-Roman, C., Ordóñez, C., Plane, J. M. C., and Saiz-Lopez, A.: Latitudinal distribution of reactive iodine in the Eastern Pacific and its link to open ocean sources, Atmos. Chem. Phys., 12, 11609–11617, https://doi.org/10.5194/acp-12-11609-2012, 2012.

McFiggans, G., Plane, J. M. C., Allan, B. J., Carpenter, L. J., Coe, H., and O'Dowd, C.: A modeling study of iodine chemistry in the marine boundary layer, J. Geophys. Res.-Atmos., 105, 14371–14385, https://doi.org/10.1029/1999jd901187, 2000.

O'Dowd, C. D., Jimenez, J. L., Bahreini, R., Flagan, R. C., Seinfeld, J. H., Hameri, K., Pirjola, L., Kulmala, M., Jennings, S. G., and Hoffmann, T.: Marine aerosol formation from biogenic iodine emissions, Nature, 417, 632–636, https://doi.org/10.1038/nature00775, 2002.

Ordóñez, C., Lamarque, J.-F., Tilmes, S., Kinnison, D. E., Atlas, E. L., Blake, D. R., Sousa Santos, G., Brasseur, G., and Saiz-Lopez, A.: Bromine and iodine chemistry in a global chemistry-climate model: description and evaluation of very short-lived oceanic sources, Atmos. Chem. Phys., 12, 1423–1447, https://doi.org/10.5194/acp-12-1423-2012, 2012.

Platt, U. and Stutz, J.: Differential Optical Absorption Spectroscopy, Physics of Earth and Space Environments, Springer-Verlag Berlin Heidelberg, https://doi.org/10.1007/978-3-540-75776-4, 2008.

Pound, R. J., Sherwen, T., Helmig, D., Carpenter, L. J., and Evans, M. J.: Influences of oceanic ozone deposition on tropospheric photochemistry, Atmos. Chem. Phys., 20, 4227–4239, https://doi.org/10.5194/acp-20-4227-2020, 2020.

Prados-Roman, C., Cuevas, C. A., Hay, T., Fernandez, R. P., Mahajan, A. S., Royer, S.-J., Galí, M., Simó, R., Dachs, J., Großmann,

K., Kinnison, D. E., Lamarque, J.-F., and Saiz-Lopez, A.: Iodine oxide in the global marine boundary layer, Atmos. Chem. Phys., 15, 583–593, https://doi.org/10.5194/acp-15-583-2015, 2015a.

Prados-Roman, C., Cuevas, C. A., Fernandez, R. P., Kinnison, D. E., Lamarque, J.-F., and Saiz-Lopez, A.: A negative feedback between anthropogenic ozone pollution and enhanced ocean emissions of iodine, Atmos. Chem. Phys., 15, 2215–2224, https://doi.org/10.5194/acp-15-2215-2015, 2015b.

Read, K. A., Mahajan, A. S., Carpenter, L. J., Evans, M. J., Faria, B. V. E., Heard, D. E., Hopkins, J. R., Lee, J. D., Moller, S. J., Lewis, A. C., Mendes, L., McQuaid, J. B., Oetjen, H., Saiz-Lopez, A., Pilling, M. J., and Plane, J. M. C.: Extensive halogen-mediated ozone destruction over the tropical Atlantic Ocean, Nature, 453, 1232–1235, https://doi.org/10.1038/nature07035, 2008.

Rex, M., Wohltmann, I., Ridder, T., Lehmann, R., Rosenlof, K., Wennberg, P., Weisenstein, D., Notholt, J., Krüger, K., Mohr, V., and Tegtmeier, S.: A tropical West Pacific OH minimum and implications for stratospheric composition, Atmos. Chem. Phys., 14, 4827–4841, https://doi.org/10.5194/acp-14-4827-2014, 2014.

Riffault, V., Bedjanian, Y., and Poulet, G.: Kinetic and mechanistic study of the reactions of OH with IBr and HOI, J. Photoch. Photobio. A, 176, 155–161, https://doi.org/10.1016/j.jphotochem.2005.09.002, 2005.

Rothman, L. S., Gordon, I. E., Babikov, Y., Barbe, A., Benner, D. C., Bernath, P. F., Birk, M., Bizzocchi, L., Boudon, V., Brown, L. R., Campargue, A., Chance, K., Cohen, E. A., Coudert, L. H., Devi, V. M., Drouin, B. J., Fayt, A., Flaud, J. M., Gamache, R. R., Harrison, J. J., Hartmann, J. M., Hill, C., Hodges, J. T., Jacquemart, D., Jolly, A., Lamouroux, J., Le Roy, R. J., Li, G., Long, D. A., Lyulin, O. M., Mackie, C. J., Massie, S. T., Mikhailenko, S., Muller, H. S. P., Naumenko, O. V., Nikitin, A. V., Orphal, J., Perevalov, V., Perrin, A., Polovtseva, E. R., Richard, C., Smith, M. A. H., Starikova, E., Sung, K., Tashkun, S., Tennyson, J., Toon, G. C., Tyuterev, V. G., and Wagner, G.: The HITRAN2012 molecular spectroscopic database, J. Quant. Spectrosc. Ra., 130, 4–50, https://doi.org/10.1016/j.jqsrt.2013.07.002, 2013.

Rowley, D. M., Mössinger, J. C., Cox, R. A., and Jones, R.L .: The UV-visible absorption cross-sections and atmospheric photolysis rate of HOI, J. Atmos. Chem., 34, 137–151, 1999.

Saiz-Lopez, A., Lamarque, J.-F., Kinnison, D. E., Tilmes, S., Ordóñez, C., Orlando, J. J., Conley, A. J., Plane, J. M. C., Mahajan, A. S., Sousa Santos, G., Atlas, E. L., Blake, D. R., Sander, S. P., Schauffler, S., Thompson, A. M., and Brasseur, G.: Estimating the climate significance of halogen-driven ozone loss in the tropical marine troposphere, Atmos. Chem. Phys., 12, 3939–3949, https://doi.org/10.5194/acp-12-3939-2012, 2012.

Saiz-Lopez, A., Fernandez, R. P., Ordóñez, C., Kinnison, D. E., Gómez Martín, J. C., Lamarque, J.-F., and Tilmes, S.: Iodine chemistry in the troposphere and its effect on ozone, Atmos. Chem. Phys., 14, 13119–13143, https://doi.org/10.5194/acp-14-13119-2014, 2014.

Saiz-Lopez, A., Baidar, S., Cuevas, C. A., Koenig, T. K., Fernandez, R. P., Dix, B., Kinnison, D. E., Lamarque, J. F., Rodriguez-Lloveras, X., Campos, T. L., and Volkamer, R.: Injection of iodine to the stratosphere, Geophys. Res. Lett., 42, 6852–6859, https://doi.org/10.1002/2015gl064796, 2015.

Saiz-Lopez, A., Plane, J. M. C., Cuevas, C. A., Mahajan, A. S., Lamarque, J.-F., and Kinnison, D. E.: Nighttime atmospheric

chemistry of iodine, Atmos. Chem. Phys., 16, 15593–15604, https://doi.org/10.5194/acp-16-15593-2016, 2016.

Sakamoto, Y., Yabushita, A., Kawasaki, M., and Enami, S.: Direct emission of I$_2$ molecule and IO radical from the heterogeneous reactions of gaseous ozone with aqueous potassium iodide solution, J. Phys. Chem. A, 113, 7707–7713, https://doi.org/10.1021/jp903486u, 2009.

Sander, S. P., Friedl, R. R., Abbatt, J. P. D., Barker, J. R., Burkholder, J. B., Golden, D. M., Kolb, C. E., Kurylo, M. J., Moortgat, G. K., Wine, P. H., Huie, R. E., and Orkin, V. L.: Chemical kinetics and photochemical data for use in atmospheric studies, Evaluation Number 17, Tech. rep., NASA Jet Propulsion Laboratory, 2011.

Seery, D. J. and Britton, D.: The continuous absorption spectra of chlorine, bromine, bromine chloride, iodine chloride, and iodine bromide, J. Phys. Chem., 68, 2263–2266, 1964.

Sekiya, T., Kanaya, Y., Sudo, K., Taketani, F., Iwamoto, Y., Aita, M. N., Yamamoto, A., and Kawamoto, K.: Global Bromine- and Iodine-Mediated Tropospheric Ozone Loss Estimated Using the CHASER Chemical Transport Model, Sola, 16, 220–227, https://doi.org/10.2151/sola.2020-037, 2020.

Shaw, M. D. and Carpenter, L. J.: Modification of Ozone Deposition and I-2 Emissions at the Air-Aqueous Interface by Dissolved Organic Carbon of Marine Origin, Environ. Sci. Technol., 47, 10947–10954, https://doi.org/10.1021/es4011459, 2013.

Sherwen, T., Schmidt, J. A., Evans, M. J., Carpenter, L. J., Großmann, K., Eastham, S. D., Jacob, D. J., Dix, B., Koenig, T. K., Sinreich, R., Ortega, I., Volkamer, R., Saiz-Lopez, A., Prados-Roman, C., Mahajan, A. S., and Ordóñez, C.: Global impacts of tropospheric halogens (Cl, Br, I) on oxidants and composition in GEOS-Chem, Atmos. Chem. Phys., 16, 12239–12271, https://doi.org/10.5194/acp-16-12239-2016, 2016.

Sherwen, T., Evans, M. J., Carpenter, L. J., Schmidt, J. A., and Mickley, L. J.: Halogen chemistry reduces tropospheric O$_3$ radiative forcing, Atmos. Chem. Phys., 17, 1557–1569, https://doi.org/10.5194/acp-17-1557-2017, 2017.

Simpson, W. R., Brown, S. S., Saiz-Lopez, A., Thornton, J. A., and von Glasow, R.: Tropospheric Halogen Chemistry: Sources, Cycling, and Impacts, Chem. Rev., 115, 4035–4062, https://doi.org/10.1021/cr5006638, 2015.

Sinreich, R., Frieß, U., Wagner, T., and Platt, U.: Multi axis differential optical absorption spectroscopy (MAX-DOAS) of gas and aerosol distributions, Faraday Discuss., 130, 153–164; https://doi.org/10.1039/b419274p, 2005.

Sipila, M., Sarnela, N., Jokinen, T., Henschel, H., Junninen, H., Kontkanen, J., Richters, S., Kangasluoma, J., Franchin, A., Perakyla, O., Rissanen, M. P., Ehn, M., Vehkamaki, H., Kurten, T., Berndt, T., Petaja, T., Worsnop, D., Ceburnis, D., Kerminen, V. M., Kulmala, M., and O'Dowd, C.: Molecular-scale evidence of aerosol particle formation via sequential addition of HIO$_3$, Nature, 537, 532–534, https://doi.org/10.1038/nature19314, 2016.

Spurr, R. J. D.: VLIDORT: A linearized pseudo-spherical vector discrete ordinate radiative transfer code for forward model and retrieval studies in multilayer multiple scattering media, J. Quant. Spectrosc. Ra., 102, 316–342, https://doi.org/10.1016/j.jqsrt.2006.05.005, 2006.

Stockwell, W. R., Kirchner, F., Kuhn, M., and Seefeld, S.: A new mechanism for regional atmospheric chem-

istry modeling, J. Geophys. Res.-Atmos., 102, 25847–25879, https://doi.org/10.1029/97jd00849, 1997.

Stutz, J., Hebestreit, K., Alicke, B., and Platt, U.: Chemistry of halogen oxides in the troposphere: Comparison of model calculations with recent field data, J. Atmos. Chem., 34, 65–85, https://doi.org/10.1023/A:1006245802825, 1999.

Takashima, H., Shiotani, M., Fujiwara, M., Nishi, N., and Hasebe, F.: Ozonesonde observations at Christmas Island (2 degrees N, 157 degrees W) in the equatorial central Pacific, J. Geophys. Res.-Atmos., 113, D10112, https://doi.org/10.1029/2007jd009374, 2008.

Takashima, H., Irie, H., Kanaya, Y., Shimizu, A., Aoki, K., and Akimoto, H.: Atmospheric aerosol variations at Okinawa Island in Japan observed by MAX-DOAS using a new cloud-screening method, J. Geophys. Res.-Atmos., 114, D18213, https://doi.org/10.1029/2009jd011939, 2009.

Takashima, H., Irie, H., Kanaya, Y., and Akimoto, H.: Enhanced NO$_2$ at Okinawa Island, Japan caused by rapid air-mass transport from China as observed by MAX-DOAS, Atmos. Environ., 45, 2593–2597, https://doi.org/10.1016/j.atmosenv.2010.10.055, 2011.

Takashima, H., Irie, H., Kanaya, Y., and Syamsudin, F.: NO$_2$ observations over the western Pacific and Indian Ocean by MAX-DOAS on *Kaiyo*, a Japanese research vessel, Atmos. Meas. Tech., 5, 2351–2360, https://doi.org/10.5194/amt-5-2351-2012, 2012.

Takashima, H., Kanaya, Y., and Taketani, F.: Downsizing of a ship-borne MAX-DOAS instrument, JAMSTEC Report of Research and Development, 23, 34–40, https://doi.org/10.5918/jamstecr.23.34, 2016.

Tellinghuisen, J.: Resolution of the visible-infrared absorption spectrum of I$_2$ into three contributing transitions, J. Chem. Phys., 58, 2821–2834, 1973.

Thalman, R. and Volkamer, R.: Temperature dependent absorption cross-sections of O-2-O-2 collision pairs between 340 and 630 nm and at atmospherically relevant pressure, Phys. Chem. Chem. Phys., 15, 15371–15381, https://doi.org/10.1039/c3cp50968k, 2013.

Tinel, L., Adams, T. J., Hollis, L. D. J., Bridger, A. J. M., Chance, R. J., Ward, M. W., Ball, S. M., and Carpenter, L. J.: Influence of the Sea Surface Microlayer on Oceanic Iodine Emissions, Environ. Sci. Technol., 54, 13228–13237, https://doi.org/10.1021/acs.est.0c02736, 2020.

Tirpitz, J.-L., Frieß, U., Hendrick, F., Alberti, C., Allaart, M., Apituley, A., Bais, A., Beirle, S., Berkhout, S., Bognar, K., Bösch, T., Bruchkouski, I., Cede, A., Chan, K. L., den Hoed, M., Donner, S., Drosoglou, T., Fayt, C., Friedrich, M. M., Frumau, A., Gast, L., Gielen, C., Gomez-Martín, L., Hao, N., Hensen, A., Henzing, B., Hermans, C., Jin, J., Kreher, K., Kuhn, J., Lampel, J., Li, A., Liu, C., Liu, H., Ma, J., Merlaud, A., Peters, E., Pinardi, G., Piters, A., Platt, U., Puentedura, O., Richter, A., Schmitt, S., Spinei, E., Stein Zweers, D., Strong, K., Swart, D., Tack, F., Tiefengraber, M., van der Hoff, R., van Roozendael, M., Vlemmix, T., Vonk, J., Wagner, T., Wang, Y., Wang, Z., Wenig, M., Wiegner, M., Wittrock, F., Xie, P., Xing, C., Xu, J., Yela, M., Zhang, C., and Zhao, X.: Intercomparison of MAX-DOAS vertical profile retrieval algorithms: studies on field data from the CINDI-2 campaign, Atmos. Meas. Tech., 14, 1–35, https://doi.org/10.5194/amt-14-1-2021, 2021.

Tsunogai, S. and Henmi, T.: Iodine in the surface water of the ocean, J. Ocean. Soc. Jpn., 27, 67–72, https://doi.org/10.1007/BF02109332, 1971.

Vandaele, A. C., Hermans, C., Simon, P. C., Carleer, M., Colin, R., Fally, S., Merienne, M. F., Jenouvrier, A., and Coquart, B.: Measurements of the NO_2 absorption cross-section from $42\,000\,cm^{-1}$ to $10\,000\,cm^{-1}$ (238–1000 nm) at 220 K and 294 K, J. Quant. Spectrosc. Ra., 59, 171–184, https://doi.org/10.1016/S0022-4073(97)00168-4, 1998.

Volkamer, R., Coburn, S., Dix, B., and Sinreich, R.: MAX-DOAS observations from ground, ship, and research aircraft: maximizing signal-to-noise to measure "weak" absorbers, Proc. SPIE, 7462, 746203, https://doi.org/10.1117/12.826792, 2009.

Volkamer, R., Baidar, S., Campos, T. L., Coburn, S., DiGangi, J. P., Dix, B., Eloranta, E. W., Koenig, T. K., Morley, B., Ortega, I., Pierce, B. R., Reeves, M., Sinreich, R., Wang, S., Zondlo, M. A., and Romashkin, P. A.: Aircraft measurements of BrO, IO, glyoxal, NO_2, H_2O, O_2–O_2 and aerosol extinction profiles in the tropics: comparison with aircraft-/ship-based in situ and lidar measurements, Atmos. Meas. Tech., 8, 2121–2148, https://doi.org/10.5194/amt-8-2121-2015, 2015.

von Glasow, R.: Modeling the gas and aqueous phase chemistry of the marine boundary layer, PhD Thesis, Johannes Gutenberg-Univertsität, Mainz, Germany, 2000.

Wagner, T., Dix, B., von Friedeburg, C., Frieß, U., Sanghavi, S., Sinreich, R., and Platt, U.: MAX-DOAS O-4 measurements: A new technique to derive information on atmospheric aerosols – Principles and information content, J. Geophys. Res.-Atmos., 109, D22205, https://doi.org/10.1029/2004jd004904, 2004.

Watanabe, K., Matsuda, S., Cuevas, C. A., Saiz-Lopez, A., Yabushita, A., and Nakano, Y.: Experimental Determination of the Photooxidation of Aqueous I- as a Source of Atmospheric I-2, ACS Earth Space Chem., 3, 669–679, https://doi.org/10.1021/acsearthspacechem.9b00007, 2019.

Wittrock, F., Oetjen, H., Richter, A., Fietkau, S., Medeke, T., Rozanov, A., and Burrows, J. P.: MAX-DOAS measurements of atmospheric trace gases in Ny-Ålesund – Radiative transfer studies and their application, Atmos. Chem. Phys., 4, 955–966, https://doi.org/10.5194/acp-4-955-2004, 2004.

Zhao, X., Hou, X. L., and Zhou, W. J.: Atmospheric Iodine (I-127 and I-129) Record in Spruce Tree Rings in the Northeast Qinghai-Tibet Plateau, Environ. Sci. Technol., 53, 8706–8714, https://doi.org/10.1021/acs.est.9b01160, 2019.